STATE OF STRESS AT THE SOUTHERNMOST END OF THE SAN ANDREAS FAULT: INTEGRATION OF SEISMICITY PATTERNS AND FOCAL MECHANISMS WITH FAULT STRUCTURE OBSERVED IN SEISMIC REFLECTION DATA BENEATH THE SALTON SEA

G09AP00098

Award Period: 01 July 2009 – 30 June 2010

Dr. Debi Kilb

Scripps Institution of Oceanography/IGPP MC 0225
University of California, San Diego
La Jolla, California 92093-0225 USA
Tele: (858) 822-4607; FAX: (858) 534-6354
E-mail: dkilb@ucsd.edu

Research supported by the U.S. Geological Survey (USGS), Department of the Interior, under USGS award number G09AP00098. *The views and conclusions contained in this document are those of the authors and should not be interpreted as necessarily representing the official policies, either expressed or implied, of the U.S. Government.*

STATE OF STRESS AT THE SOUTHERNMOST END OF THE SAN ANDREAS FAULT: INTEGRATION OF SEISMICITY PATTERNS AND FOCAL MECHANISMS WITH FAULT STRUCTURE OBSERVED IN SEISMIC REFLECTION DATA BENEATH THE SALTON SEA

Technical Abstract

The southern San Andreas Fault (SSAF) in California has not had a large earthquake in approximately 300 years, yet the average recurrence for the previous five ruptures is about 180 years (Philibosian *et al*., 2010). A 60 km section of the SSAF periodically has been submerged during high-stands of the large late-Holocene Lake Cahuilla (LC), and emerging evidence indicates coincident timing between LC flooding and fault displacement. As a large SSAF earthquake appears imminent, it is important to understand how crustal stress perturbations can promote or inhibit fault failure(s). Here, we assess the potential for LC to act as a catalyst in triggering a sequence of large earthquakes. Model results of static Coulomb stress perturbations indicate the additive stress changes from lake loading (up to 0.4 MPa) and normal fault displacement (up to 1.4 MPa) are sufficiently high to potentially trigger an earthquake on the SSAF, particularly if a single lake filling event triggers rupture of several normal faults, as the stratigraphic records suggest. Since the current lake level is relatively stable, any future interaction between the faults under today's Salton Sea and the SSAF will depend solely on tectonic loading, without any perturbing stresses from lake level changes. These results highlight the importance of including lake loading and secondary fault ruptures in seismic hazard assessments, as both have the potential to modulate earthquake cycles on major plate boundary faults such as the SSAF.

Non-Technical Abstract

This work address two fundamental, yet unanswered, questions about the southern San Andreas Fault (SSAF) in California: (1) Why has the SSAF not produced a large earthquake rupture in ~300 years, even though the average recurrence for the last five earthquakes is ~180 years; and (2) What mechanism can explain the twenty years of research that show an apparent correlation between high-stands of Lake Cahuilla and large earthquake ruptures on the SSAF. We propose that prehistoric flooding of Lake Cahuilla (which encompassed an area significantly larger than the present day Salton Sea) may have been a catalyst in triggering a sequence of large earthquakes in Southern California in the past. One of the most plausible sequences is that stresses generated by the lake-load promote rupture on faults beneath the lake, and these in turn promote rupture on the SSAF. Geological observations and theoretical stress models suggest that the role of both the lake level and rupture of faults beneath the lake are an important component in this triggering sequence. This suggests that a large rupture on the SSAF has likely been delayed because of the absence of extensive Lake-loading within the last 300 years.

Introduction

The most robust paleoseismic history on the SSAF (Philibosian *et al*., 2010) is recorded in sediment deposited during transgressive and regressive cycles of ancient Lake Cahuilla (LC), a large inland lake that formed episodically as a result of northward diversions of the Colorado River into the Salton Trough (Figure 1). Throughout the late Holocene the Salton Trough was episodically inundated with Colorado River water to form ancient Lake Cahuilla, flooding to heights of ~13 m above sea level within periods of 20 years or less (Waters, 1983).

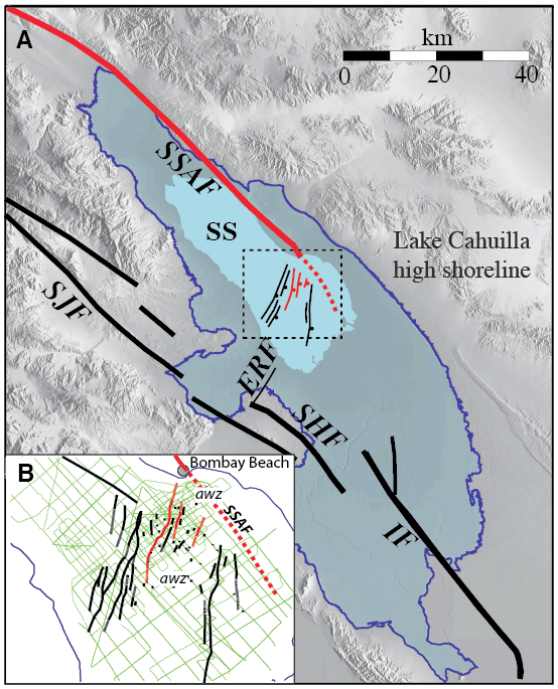

Figure 1. ***(A)*** *Study region near the Salton Sea (SS), which is a man-made lake partially filling the basin containing ancient Lake Cahuilla (blue line indicates high shoreline). Active faults are shown (black and red lines, red denoting faults discussed in this study), including the Southern San Andreas Fault (SSAF) and a series of N15°E trending normal faults under the Salton Sea. Abbreviations: San Jacinto Fault, SJF; Elmore Ranch Fault, ERF; Superstition Hills Fault, SHF; Imperial Fault, IF.* ***(B)*** *Location map of seismic reflection profiles (green lines). Sub-bottom imagery was limited in areas of high surficial gas, creating acoustic wipe-out zones (awz).*

Although some studies show evidence of concurrent timing and recurrence intervals between Lake Cahuilla highstands and earthquakes on the SSAF (Brothers *et al*., 2009; Philibosian *et al*., 2010), the causal mechanism between lake filling and fault rupture remains unclear. Recent viscoelastic modeling of the effects of Lake Cahuilla loading on dextral strike-slip faults in the Salton Sea region, oriented similarly to the SSAF, could not provide firm conclusions about the potential link between lake load and earthquake triggering on the SSAF (Luttrell *et al*., 2007). However, these models did not incorporate the recently discovered host of normal faults under the Salton Sea that have down-to-the-southeast displacement (Brothers *et al*., 2009). These newly identified faults trend ~N15°E, have slip-rates greater than 1 mm/yr and many appear to be kinematically linked to the SSAF.

As a large earthquake on the SSAF may be imminent, it is important to understand how crustal stress perturbations, both tectonic and lake loading, can promote or inhibit fault failure. Here, we use geologic and seismic observations to constrain static stress change models in order to test the hypothesis that prehistoric flooding of LC (which encompassed an area significantly larger than the present day Salton Sea) may have been a catalyst in triggering a sequence of large earthquakes in Southern California

in the past. From our model results, we suggest Lake Cahuilla flooding may have induced failure on normal faults below the Salton Sea, which, in turn, could have the potential to trigger earthquake rupture on the SSAF.

Results

Assessing fault complexity: We identify linear and planar trends in geologic and seismologic data and catalog estimates of fault strike and dip using, when appropriate, principal component analysis (MATLAB routine PCACOV). From the relocated seismicity data (Lin *et al.,* 2007) we find primarily vertical faulting with assumed strike slip motion (Table 1). One group of these faults map a 'rung and ladder' pattern with multiple liniments striking ~N45°E (Fault ID's S1, S2, S3, S4; see Table 1), orientations approximately perpendicular to the southern SAF. We assume these faults have a left-lateral sense of slip, which is consistent with focal mechanism data and the tectonically loaded background stress field (Hardebeck & Hauksson, 1999). The geologic seismic reflection data, however, presents fault strikes of ~N15°E dipping ~65° to the southeast with normal fault motion. The complexity of fault patterns within our study region leads to different tectonic interpretations (Nicholson *et al.,* 1986; Brothers *et al.,* 2009). The short, northeast oriented lineaments in the rung-and-ladder pattern may simply represent a transition zone between the end of the SSAF and the SSAF-Imperial Fault pull-apart basin, whereas the orientations of the newly discovered normal faults beneath the Sea are consistent with the direction of opening predicted by plate motion vectors (Brothers *et al.,* 2009).

Table 1. *Identifying small-scale fault orientations. To identify fault strike and dip within subsets of the relocated earthquake data we use principal component analysis (MATLAB routine PCACOV).*

Fault ID	Median Location (lon, lat, depth in km)	Data Type	Number of Earthquakes	Strike	Dip
H7	(-115.75, 33.27, -3.0)	seismic reflection	--	N30°E	65°
E2	(-115.70, 33.21, -3.0)	seismic reflection	--	N10°E	65°
N2	(-116.03, 33.45, -3.0)	seismic reflection	--	N07°E	65°
S1	(-115.73, 33.31, -6.9)	relocated seismicity	147	N44°E	88°
S2	(-115.78, 33.30, -6.6)	relocated seismicity	159	N45°E	89°
S3	(-115.71, 33.29, -7.0)	relocated seismicity	335	N50°E	89°
S4	(-115.69, 33.31, -7.6)	relocated seismicity	368	N36°W	86°
S11	(-115.64, 33.17, -6.6)	relocated seismicity	305	N2°E	85°
S12	(-115.61, 33.17, -6.2)	relocated seismicity	327	N52°E	89°
SAF	(-115.71, 33.35, -6.0)	approximated from the Community Fault Model (Plesch *et al.,* 2007)	--	N45°W	90°

Modeling Static Stress Changes Caused by Lake Cahuilla flooding: Studies have shown that pore pressure changes from lake filling (Simpson *et al.,* 1988) and static stress loading from fault displacement (Hudnut *et al.,* 1989; King *et al.,* 1994; Aron &

Hardebeck, 2009; Parsons & Velasco, 2009) have been associated with earthquake triggering and increased seismicity. Using data from our study region we investigate both of these models focusing on earthquake triggering scenarios involving large lake loads, earthquake rupture on normal faults beneath the Sea and earthquake rupture on the SSAF. We also assess the uncertainties in our results.

To investigate the effects of Lake Cahuilla flooding, we estimate the static stress changes induced by mechanical deformation in response to the weight of the lake water on an elastic plate overlying a viscoelastic halfspace and perturbations to effective normal stresses via a hydrostatic increase in pore pressure at depth (King *et al.,* 1994; Cartwright *et al.,* 1998; Luttrell *et al.,* 2007; Luttrell and Sandwell, 2010). Our models assume a lake level history with a constant influx at a conservative filling rate that fills the lake from dry to 13 m in 20 years (Waters, 1983). Static stress from increasing pore pressure from the lake load is calculated as:

$$\Delta CFS^{pore\ pressure} = \mu' \rho_w g h \qquad (1)$$

where ρ_w is the water density, g is the acceleration of gravity, h is the lake water depth, and μ' is the effective fault friction coefficient. This is the hydrostatic end member, which is independent of fault orientation and presumes pore fluids permeate hydrostatically to seismogenic depth, and should therefore be considered a maximum. Stresses induced by mechanical deformation in response to the weight of the lake water are computed in an elastic plate overlying a Maxwell viscoelastic halfspace (Luttrell *et al.,* 2007; Luttrell & Sandwell, 2010). Model parameters assume a 35 km plate and a halfspace relaxation period of 30 years, corresponding to a viscosity of 1.3e19 Pa s.

In response to a lake-filling event, we examine two faulting scenarios. The first resolves stresses on normal faults under the Sea striking N15ºE and dipping 65ºSE (See Figure 1). The second resolves stresses on vertical dextral faults striking N35ºW, similar to the SSAF. Stresses are computed at 7 km depth, which is the median seismogenic depth for this region (Nazareth & Hauksson, 2004), using a coefficient of friction of 0.4. During the first 5 years of lake filling, we find deformation in the lake region increases ΔCFS on the normal faults 0.03 MPa and decreases it 0.05 MPa on the SSAF (Figure 2).

These stresses are not by themselves enough to either trigger or obstruct a rupture on either fault. However, during the same time the elevated pore pressure induced by the lake load will increase ΔCFS by 0.18 MPa on the normal faults and 0.08 MPa on the SSAF. This assumes the pore pressure increases hydrostatically at seismogenic depth, which is an upper bound. If the pore pressure at depth increases by at least half of the hydrostatic load within the first 5 years, the increase in ΔCFS on the normal fault will exceed 0.1 MPa (a value consistent with observed aftershock triggering King *et al.,* 1994). During that same 5-year initial time period, ΔCFS will remain about the same on the SSAF (Figure 2d). As lake filling continues, ΔCFS will increase to up to 0.4 MPa on the normal faults and 0.1 MPa on the SSAF. After lake filling ceases, ΔCFS on both faults will decay as viscous rebound processes relax the asthenosphere in response to the new load.

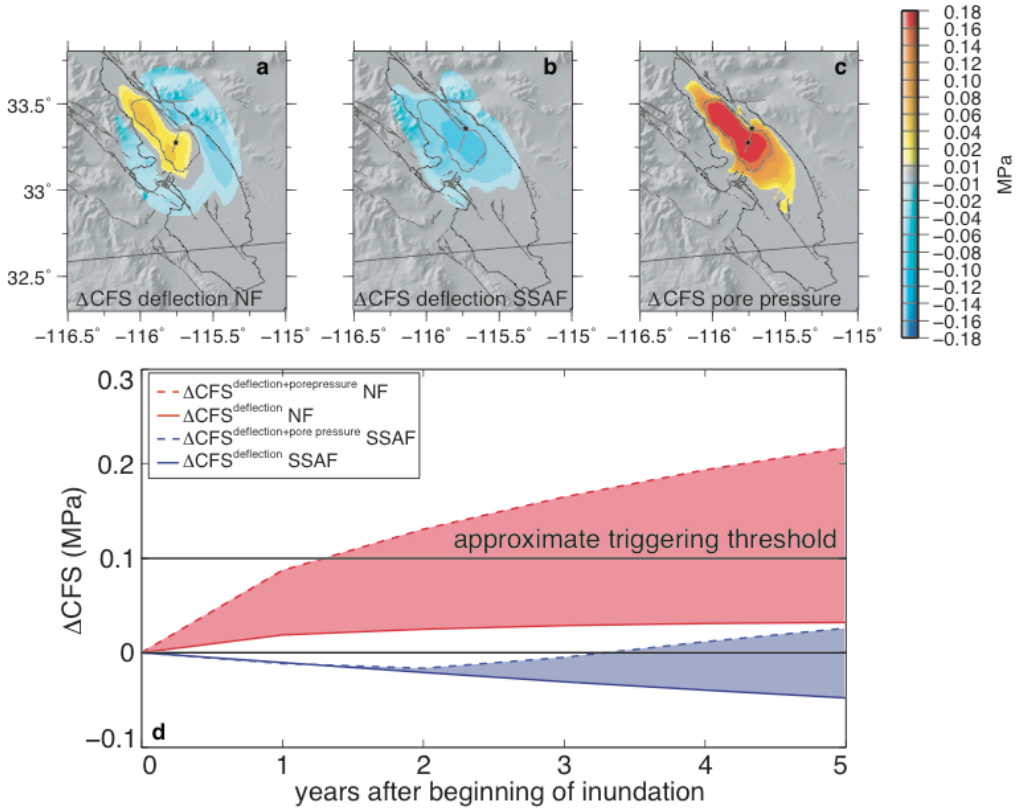

Figure 2. *Maps of static Coulomb stress (ΔCFS) models from lake loading. ΔCFS calculated from Lake Cahuilla inundation (highstand at 13 m above sea level indicated by solid black line) 5 years into the lake filling process (fills completely in 20 years) using a frictional coefficient of 0.4 for:* ***(a)*** *loading from mechanical bending derived at a depth of 7 km and resolved onto normal fault (NF) planes striking N15°E and dipping 65° SE; and* ***(b)*** *resolved on SSAF-type vertical dextral strike-slip planes striking N35°W.* ***(c)*** *ΔCFS from hydrostatic pore pressure changes based on the depth of the water (maximum end member).* ***(d)*** *ΔCFS during first five years of lake filling on the normal fault (NF) and the SSAF (exact position indicated by the stars in sub-figures a-c). Range of possible ΔCFS shown, from the minimum (stress affected by mechanical deformation only) to the maximum (stress affected by both mechanical deformation and full hydrostatic pore pressure at seismogenic depth). Black line indicates an approximate earthquake-triggering threshold.*

Modeling Static Stress Changes from Earthquakes on Normal Faults under the Salton Sea: We next investigate the causal relationship between earthquakes on the normal faults under the Salton Sea and earthquakes on the SSAF. Although dynamic stress changes likely play a role in earthquake triggering sequences (*e.g.*, Kilb *et al.*, 2000; Kilb 2003; Hill & Prejean, 2007; Hill 2008), for our purposes it is sufficient to study instantaneous static stress changes and their likelihood to facilitate rupture along the SSAF (Parsons & Velasco, 2009). We model static Coulomb stress changes (ΔCFS) induced by earthquake rupture using the Coulomb-3 software code (Okada, 1992; Lin & Stein, 2004; Toda *et al.*, 2005).

These calculations require input geometry and slip of the source faults (*i.e.*, faults that impart stresses) and the geometry of the receiver faults (*i.e.*, faults that do not slip but upon which the stresses imparted by the source faults are derived). For each receiver fault, static Coulomb failure stress change is defined as:

$$\Delta CFS = \Delta\tau + \mu'\Delta\sigma_n \qquad (2)$$

where τ is shear stress (positive in the direction of receiver fault slip), σ_n the stress normal to the fault (positive when the receiver fault is unclamped), and μ' is the effective fault friction coefficient on the receiver fault (Okada, 1992; Lin & Stein, 2004; Toda *et al.*, 2005). Coulomb stress, therefore, is a linear combination of shear stress and normal stress, modulated by the friction coefficient that can range from 0 (no friction) to 1 (high friction).

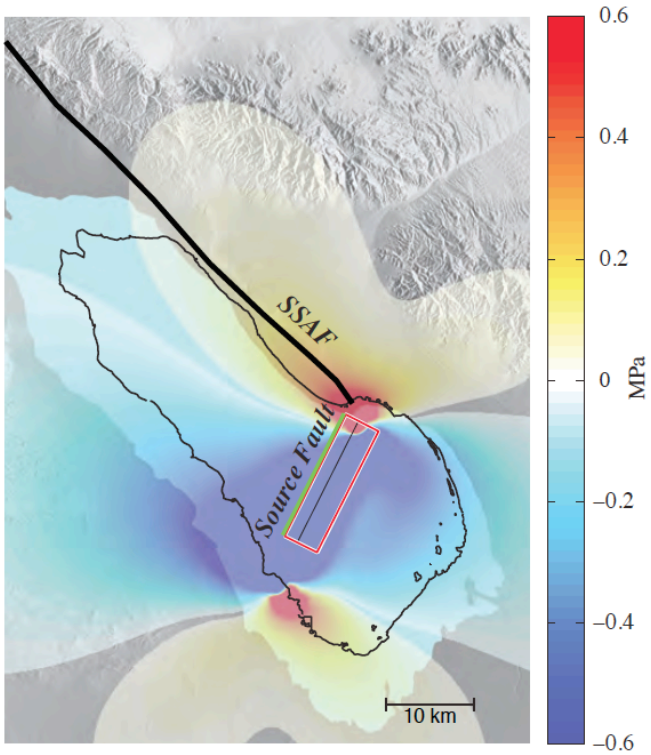

Figure 3. *Map of Coulomb static stress change. Static Coulomb stresses at a depth of 4 km generated by rupture of an extensional fault (green line shows surface trace; red rectangle shows the extrapolated fault plane; black line shows the calculation depth) embedded in an elastic half-space, using a friction coefficient of 0.6. The simulation applies 1.0 m of normal displacement to a 65°SE dipping plane that is 15 km long and 8 km deep. Resulting stresses are derived on fault planes oriented similar to the SSAF (strike=325; dip = 90; rake = 180°). Warm colors indicate areas where failure is promoted and cool colors where failure is inhibited. Stress lobes are saturated at ±0.6 MPa.*

We constrain the source fault parameters (*i.e.*, strike, dip, rake and displacement) using displacement per event measurements from CHIRP profiles in combination with results from paleoseismic reconstructions. These suggest the normal faults beneath the Sea collectively accommodate at least 50% of the SSAF strain budget and rupture every 100-300 years with 0.5-1.0 m of dip-slip displacement (Brothers *et al.*, 2009). Assuming this displacement is released seismically, these would register as magnitude ~6 earthquakes (Wells *et al., 1994*). Based on these findings we estimate static stress changes from an earthquake rupture that has 1.0 m of displacement on a normal fault striking N15ºE and dipping 65ºSE beneath the Salton Sea (Figure 3). The resulting ΔCFS map shows concentrated lobes of stress that promote rupture at the ends of the mainshock fault,

including a 1.1-1.4 MPa increase along the SSAF as it steps offshore. An increase in ΔCFS of this scale would be sufficient to trigger aftershocks (*e.g.*, King *et al.*, 1994) and potentially trigger rupture on the SSAF.

Sensitivity Tests: We completed a suite of parameter sensitivity tests for both the lake loading and earthquake rupture models that addressed variations in the frictional coefficients, elastic plate thickness, depth of observation, and rupture fault location. For our purposes, these sensitivity tests indicate minimal variations in the spatial distributions of stress and their magnitudes.

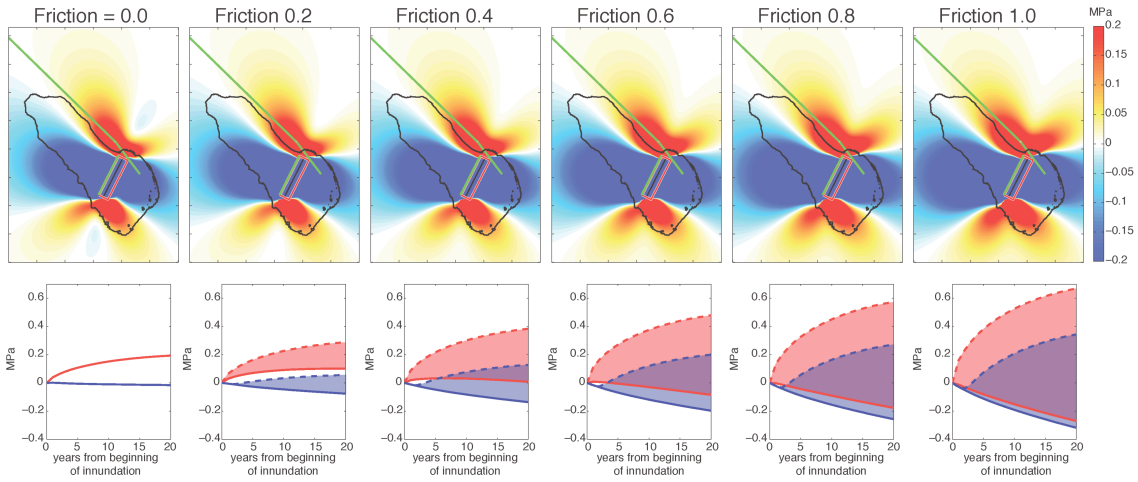

Figure 4*. (top) Static Coulomb stress from fault rupture, as in Figure 3, calculated for various effective fault friction coefficient values. Stress maps saturate at ±.2 MPa. (bottom) Static Coulomb stress changes during 20 years of LC filling, as in Figure 2d, calculated for various effective fault friction coefficient values.*

Notably, the friction coefficient minimally changes ΔCFS maps induced by earthquake rupture beneath Sea because for these calculations the of primary contribution to ΔCFS results from changes in shear stress (Figure 4: top), whereas because normal stress changes dominate the ΔCFS lake load calculations these calculations are more sensitive to variations in the selected coefficient of friction (Figure 4: bottom). We find that overall, even allowing for these variations, the models we present in this study represent a conservative selection and that our conclusions are robust to model parameter choices.

Discussion and Conclusions

Based on the ~180 year average recurrence for paleoearthquakes on the SSAF (Philibosian *et al.*, 2010) and evidence that it has continued to accumulate large amounts of strain (Fialko, 2006) since the most recent large earthquake at ~1700 AD (Seih & Williams, 1990) it is commonly believed that we are ~100 years 'overdue' for a large earthquake on the SSAF (Field *et al.*, 2009). Here, we suggest a large rupture on the SSAF has been delayed within the last 300 years because of the absence of a large lake load (*i.e.*, similar to LC), which can promote failure on the SSAF via a triggering

sequence beginning with rupture on normal faults beneath the Salton Sea. In particular we propose that capture of the Colorado River and consequent LC flooding into a dry basin provides optimal conditions for triggered rupture on normal faults beneath the lake and subsequent triggering on the SSAF. The additive static stress changes from lake loading (up to 0.4 MPa) and normal fault displacement (up to 1.4 MPa) are sufficiently high to potentially trigger an earthquake on the SSAF, particularly if a single lake filling event triggers rupture of several normal faults, as the stratigraphic records suggest (Brothers *et al.,* 2009). Because anthropogenic control of the Colorado River makes future inundation of the Salton Trough highly unlikely, we are now transitioning to a new mode of rupture dynamics where large SSAF ruptures will not be modulated by Lake Cahuilla flooding, potentially lengthening the recurrence interval between large earthquakes in southern California.

References

Aron, A., and J. L. Hardebeck, Seismicity Rate Changes along the Central California Coast due to Coulomb Stress Changes from the 2003 M6.5 San Simeon and 2004 M6.0 Parkfield Earthquakes, *Bull. Seism. Soc. Am.,* 99, 2280-2292, 2009.

Brothers, D.S., N. W. Driscoll, G. M. Kent, A. J. Harding, J. M. Babcock & R. L. Baskin, Tectonic evolution of the Salton Sea inferred from seismic reflection data. *Nature Geoscience,* 2, 581-584 (2009).

Cartwright, J., Bouroullec, R., James, D. & Johnson, H. Polycyclic motion history of some Gulf Coast growth faults from high-resolution displacement analysis. *Geology,* 26, 819-822 (1998).

Castelltort, S., Pochat, S. & Van den Driessche, J.J. Using T-Z plots as a graphical method to infer lithological variations from growth strata. *J. of Structural Geology* 26, 1425-1432 (2004).

Ferrari, R.L., "1986 Lake Powell survey" (U.S. Bureau of Reclamation Technical Report 1988).

Fialko, Y., Interseismic strain accumulation and the earthquake potential on the southern San Andreas fault system, *Nature,* 441, doi:10.1038, 968-971, (2006).

Field, E.H. T. E. Dawson, K. R. Felzer, A. D. Frankel, V. Gupta, T. H. Jordan, T. Parsons, M. D. Petersen, R. S. Stein, R. J. Weldon, and C. J. Wills, Uniform California Earthquake Rupture Forecast, Version 2 (UCERF 2). *Bull. Seismol. Soc. Am.*, 99, 2053-2107 (2009).

Hardebeck, J.L. & Shearer, P.M. Using S/P amplitude ratios to constrain the focal mechanisms of small earthquakes. *Bull. Seismol. Soc. Am.*, 93, 2434-2444 (2003).

Hardebeck, J. L. and E. Hauksson, Role of Fluids in Faulting Inferred from Stress Field Signatures, *Science,* 285, 236-239, (1999).

Harris, R. A., Introduction to special section: Stress triggers, stress shadows, and implications for seismic hazard, *J. Geophys. Res., 103*,24,347–24,358, 1998.

Hill, D.P., S. G. Prejean, (edited by Hiroo Kanamori) Volume 4 as part of the Elsevier Treatise on Geophysics Series, (2007).

Hill, D. P., Dynamic Stresses, Coulomb failure, and remote triggering, *Bull. Seismol. Soc. Am.*, 98, 66–92, 2008.

Hudnut, K.W., L. Seeber, and J. Pacheco, Cross-fault triggering in the November 1987 Superstition Hills earthquake sequence, southern California, *Geophys. Res. Lett.*, 16, pp. 199-202, (1989).

Kilb, D., J. S. Gomberg, and P. Bodin, Triggering of earthquake aftershocks by dynamic stresses, *Nature, 408*, 570-574, 2000.

Kilb, D., A strong correlation between induced peak dynamic Coulomb stress change from the 1992 M7.3 Landers earthquake and the hypocenter of the 1999 M7.1, *J. Geophys. Res.*, 108, B1, 2012, 2003.

King, G.C.P., Stein, R.S. & Lin, J. Static Stress Changes and the Triggering of Earthquakes. *Bull. Seismol. Soc. Am.*, 84, 935-953 (1994).

Lin, G.Q., Shearer, P.M. & Hauksson, E. Applying a three-dimensional velocity model, waveform cross correlation, and cluster analysis to locate southern California seismicity from 1981 to 2005. *J. Geophys. Res.,* 112, (2007).

Lin, J. & Stein, R.S. Stress triggering in thrust and subduction earthquakes and stress interaction between the southern San Andreas and nearby thrust and strike-slip faults. *J. Geophys. Res.,* 109, 10.1029/2003JB002607 (2004).

Luttrell, K. & D. Sandwell, Ocean Loading Effects on Stress at Near Shore Plate Boundary Fault Systems. *J. Geophys. Res.,* 115, B08411, doi:10.1029/2009JB006541, (2010).

Luttrell, K., Sandwell, D., Smith-Konter, B., Bills, B. & Bock, Y. Modulation of the earthquake cycle at the southern San Andreas fault by lake loading. *J. Geophys. Res.,* 112, 1029/2006JB004752 (2007).

Meltzner, A.J. & Wald, D.J. Aftershocks and triggered events of the Great 1906 California earthquake. *Bull. Seismol. Soc. Am.*, 93, 2160-2186 (2003).

Nazareth, J.J. & Hauksson, E. The seismogenic thickness of the southern California crust. *Bull. Seismol. Soc. Am.*, 94, 940-960 (2004).

Nicholson, C., L. Seeber, P. Williams, L. R. Sykes, Tectonics 5, 629 (1986).

Okada, Y. Internal Deformation Due to Shear and Tensile Faults in a Half-Space. *Bull. Seismol. Soc. Am.*, 82, 1018-1040 (1992).

Parsons, T., and A. A. Velasco, On near-source earthquake triggering, *J. Geophys. Res.*, 2009.

Philibosian, B., Fumal, T.E. & R. Weldon, San Andreas Fault earthquake chronology and Lake Cahuilla history at Coachella, California. *Bull. Seismol. Soc. Am.*, accepted (2010).

Plesch, A., J. H. Shaw, C. Benson, W. A. Bryant, S. Carena, M. Cooke, J. Dolan, G. S. Fuis, E. Gath, L. Grant, E. Hauksson, T. Jordan, M. Kamerling, M. Legg, S. Lindvall, H. Magistrale, C. Nicholson, N. Niemi, M. Oskin, S. Perry, G. Planansky, T. Rockwell, P. Shearer, C. Sorlien, M. P. Suess, J. Suppe, J. Treiman, and R. Yeats, Community Fault Model (CFM) for Southern California, *Bull. Seismol. Soc. Am.*, 97, p. 1793-1802, DOI: 10.1785/0120050211 (2007).

Sieh, K.E. & Williams, P.L. Behavior of the Southernmost San-Andreas Fault during the Past 300 Years. *J. Geophys. Res.,* 95, 6629-6645 (1990).

Simpson, D.W., Leith, W.S. & Scholz, C.H. 2 Types of Reservoir-Induced Seismicity. *Bull. Seismol. Soc. Am.*, 78, 2025-2040 (1988).

Toda, S., Stein, R.S., Richards-Dinger, K. & Bozkurt, S.B. Forecasting the evolution of seismicity in southern California: Animations built on earthquake stress

transfer. *J. Geophys. Res.,* 110, (2005).
Waters, M.R. Late Holocene Lacustrine Chronology and Archaeology of Ancient Lake Cahuilla, California. *Quaternary Research*, 19, 373-387 (1983).
Wells, D.L. and K. J. Coppersmith, *Bull. Seismol. Soc. Am.*, 84, 974 (1994).

Reports published

Brothers, D., D. Kilb, K. Luttrell, N. Driscoll, and G. Kent, "Two Potential Triggers for Large Ruptures Along the Southern San Andreas Fault: Secondary Fault Displacement and Lake Loading" Fall SCEC meeting, 2010.

Brothers, D., D. Kilb, K. Luttrell, N. Driscoll, and G. Kent, "Potential triggers for large ruptures along the southern San Andreas Fault", (In internal USGS review, 2010).

Kilb, D., D. Brothers, G. Lin, G. Kent, R. Newman and N. Driscoll, "On The Dichotomy Between Geologic and Seismologic Signatures in Data From the Salton Sea Region in Southern California", Fall SCEC meeting, 2009.

Kilb, D. L., D. S. Brothers, G. Lin, G. Kent, R. L. Newman and N. Driscoll, Faulting, Seismicity and Stress Interaction in the Salton Sea Region of Southern California", Eos Trans. AGU, V 90, Fall Meet. Suppl., Abstract T31A-1786, 2009.